D 63612

Vol. 10 Number 12

December 2013

PLASMA PROCESSES AND POLYMERS

www.plasma-polymers.org

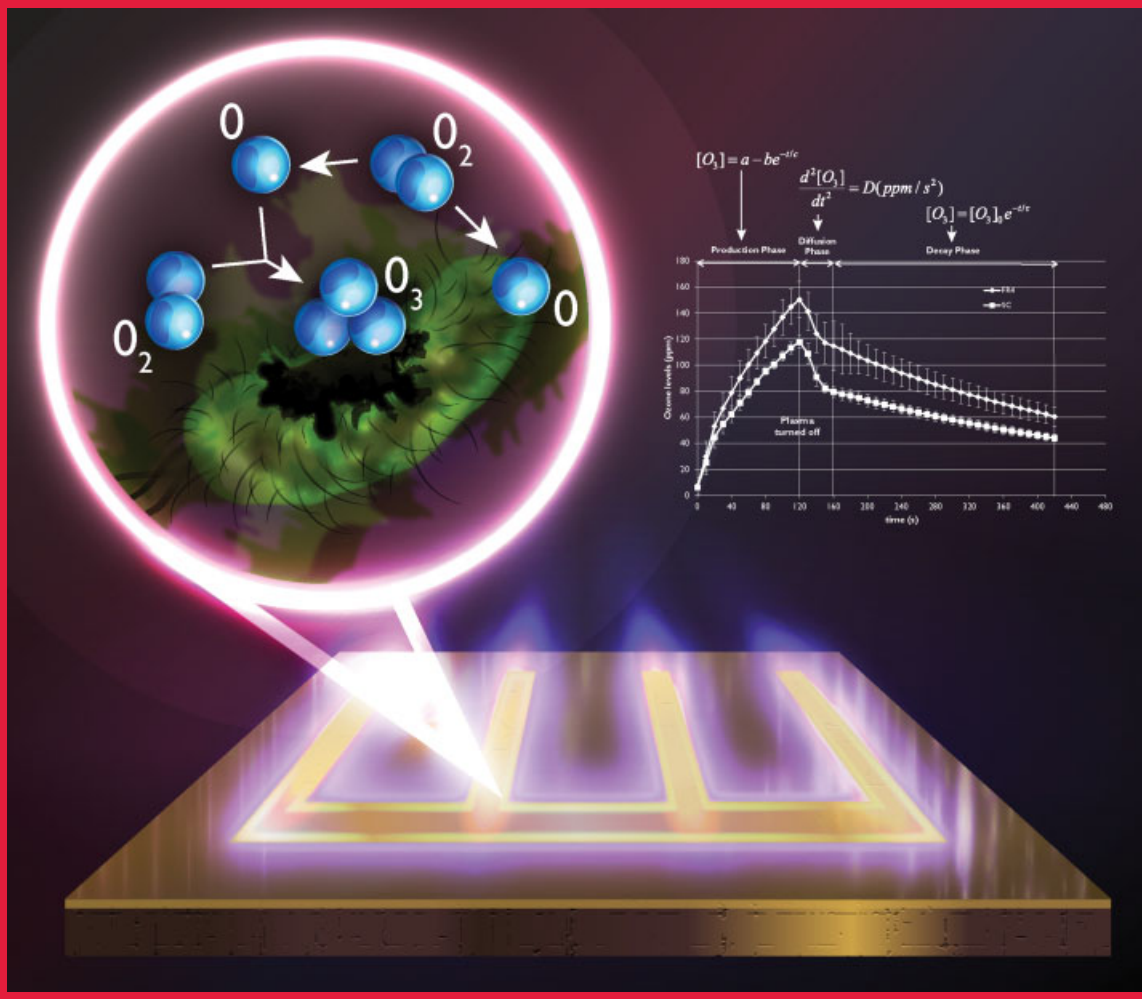

WILEY-VCH

ISSN 1612-8850 Plasma, 10, No. 12 (2013)

Examining the Role of Ozone in Surface Plasma Sterilization Using Dielectric Barrier Discharge (DBD) Plasma

Navya Mastanaiah, Poulomi Banerjee,† Judith A. Johnson, Subrata Roy*

Dielectric barrier discharge (DBD) devices are known ozone generators. Authors have previously demonstrated a DBD surface plasma source, operating in air at atmospheric pressure, to achieve killing of vegetative cells in 2–3 min and sterilization in 20 min (bacterial spores). The aim of this paper is to examine the role of the ozone in surface DBD plasma sterilization. The role of ozone in plasma killing is examined by a) characterizing the rate of production/decay of ozone during DBD plasma generation, b) studying the effect of exposing bacteria (*Escherichia coli*) solely to the ozone thus produced. Our results indicate that while ozone plays a major role, the energy flux delivered to the electrodes is also crucial in the process of plasma sterilization.

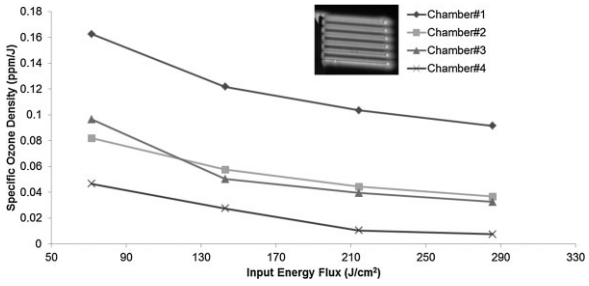

1. Introduction

Plasma sterilization offers advantages (short processing times, low operational temperatures, safety, and versatility) compared to conventional sterilization methods such as autoclaving, ethylene oxide fumigation, etc. Plasma sterilization can be classified into two types: (i) volume plasma sterilization, wherein plasma is generated between a powered and grounded electrode and contaminated samples are placed in between, so that they are immersed in the plasma, (ii) surface plasma sterilization, wherein plasma is generated atop a surface (made of a dielectric material) embedded with electrodes on either side, such that one is powered and the other is grounded. In the latter, contaminated samples are placed directly atop the surface on which plasma is generated.

Earlier experiments in plasma sterilization were mostly conducted in the low to medium pressure ranges, wherein the role of vacuum UV (VUV) radiation (wavelength <200 nm) in the process of plasma sterilization was debated.[1] During plasma generation at atmospheric pressure, the spectroscopic signature exhibits prominent intensity peaks in the wavelength range of 300–400 nm.[2,3] The intensity peaks in this wavelength range pertain mostly to transitions taking place in the 2nd positive system of nitrogen (N_2). More importantly, the spectroscopic signature of plasma at atmospheric pressure shows no intensity peaks in the wavelength range of 100–280 nm, which pertains to the UV-C regime. UV-C wavelengths are most lethal to bacterial species because of their ability to induce dimerization in the DNA of bacteria, thus arresting bacterial replication.[4] However, the absence of UV-C wavelengths in the spectroscopic signature of plasma at atmospheric pressure implies that cell damage due to UV radiation is likely not a major factor in plasma sterilization.

N. Mastanaiah, P. Banerjee, S. Roy
Department of Mechanical and Aerospace Engineering, Applied Physics Research Group (APRG), University of Florida, Gainesville, FL 32611-6300, USA
E-mail: roy@ufl.edu
J. A. Johnson
Department of Pathology, Immunology and Laboratory Medicine, College of Medicine and Emerging Pathogens Institute, University of Florida, Gainesville, FL 32610-0009, USA

†Present address: RCF Colony, Chembur, Mumbai 400074, India.

DOI: 10.1002/ppap.201300108

The other agents that might play a role in plasma sterilization are reactive chemical species (charged particles, neutrals)[5,6] and temperature.[7] The role of each of these agents in plasma sterilization remains highly debated.

The type of plasma discussed in this paper and in our previous sterilization experiments[3] is known as dielectric barrier discharge (DBD) plasma. This type of plasma is generated by applying a potential difference between two electrodes embedded on opposite sides of a dielectric (insulator) surface and is characterized by a large number of tiny filamentary micro-discharges.[8] The gap between electrodes is of the order of a few millimeters. The ease of generating DBD plasma at atmospheric pressure as well as the ability of plasma generation on surfaces makes DBD plasma ideal for applications involving surface sterilization. However, DBD plasma devices are inherent ozone generators. Hence, before DBD plasma is applied for surface sterilization technologies, it is important to characterize the trends of ozone production during DBD plasma generation as well as understand the role of ozone in DBD plasma-based sterilization. Understanding the trends of ozone production during DBD plasma generation will also provide an insight into methods required to control the amounts of ozone produced.

Ozone formation in pure oxygen (O_2) is a two-step process that starts with the dissociation of O_2 molecules by the electrons in a micro-discharge[9]

$$O_2 + e \rightarrow 2O + e \quad (1)$$

Followed by a three-body reaction

$$O + O_2 + M \rightarrow O_3 + M \quad (2)$$

where M is a third reaction partner. M can be a pure O_2 species or a N_2 species, acting as a catalyst. Ozone formation in air is slightly different from ozone formation in pure O_2, since energy provided by the electrical discharge in air is distributed between N_2 and O_2.[10] Hence in air, ozone synthesis is also influenced by contributions from N_2 in the form of mostly atomic N, which reacts with O_2 to form atomic O, which further recombines with molecular O_2 to form ozone (as shown in Equation 2). Typically, ozone formation in air takes longer than ozone formation in pure O_2.

Ozone decomposition is often coupled to ozone formation. The basic reactions for the process are[10,11]

$$\text{Decomposition}: \; O_3 + M \Leftrightarrow O_2 + O + M \quad (3)$$

$$\text{Recombination}: \; O + O_3 \rightarrow 2O_2 \quad (4)$$

Typically, when ozone dissociates and creates atomic O, the atomic O immediately reacts with molecular O_2 present to immediately form ozone. Thus, ozone formation (Equation 2) is very fast and usually able to balance ozone decomposition (Equation 3), if initial concentration of ozone is low. The ozone decomposition time depends exponentially on temperature and initial concentration of ozone.[10]

Ozone is known to have bactericidal properties. Broadwater et al.[12] determined the minimum lethal concentration of ozone in water for three bacterial species, using a contact time of 5 min. Lethal threshold concentrations for *Bacillus cereus*, *Bacillus megaterium*, and *E. coli* were determined to be 0.12, 0.19, and 0.19 mg L^{-1}, respectively, wherein 1 mg L^{-1} corresponds to 1 ppm of ozone.[1] Efremov et al.[13] discussed reaction rate constants for production and destruction of ozone formed during plasma generation. They conjectured that the antiseptic property of the excited dry air flowing out of a discharge chamber was determined by its ozone concentration and demonstrated that exposing microorganism concentrations to discharge-excited air, even for a short while, substantially reduced their amount.

Dobrynin et al.[14] pursued a different approach in isolating the role of ozone in plasma sterilization. They measured the ozone concentration produced by a DBD discharge in room air at ≈60% relative humidity as 28 ppm. Consequently, they used an ozone generator to produce the same concentration of ozone and examined the inactivation effect of this ozone concentration on *E. coli* and skin flora. They noted no inactivation. Furthermore, they also compared inactivation efficiency in two cases, one in which the measured ozone concentration was zero (DBD plasma produced in gas by diluting a mixture of nitric oxide and N_2 with O_2 gas, which inhibited ozone production) and one in which the measured ozone concentration was not zero (DBD plasma produced using a mixture of pure N_2 and O_2). They noted that the inactivation efficiency in both cases remained the same, leading them to conclude that ozone does not play a major role in bacterial inactivation.

Vaze et al.[15] used a dielectric barrier grating discharge (DBGD) to study the inactivation of airborne *E. coli* inside a closed air circulation system. They studied the effect of charged and short-lived species and the effect of ozone. They concluded from their experiments that ozone caused a reduction in bacterial load, but it may not be one of the major inactivating factors in the plasma. In contrast, comparing plasma treatment of mammalian breast epithelial cells with ozone treatment, Kalghatgi et al.[16] found that ozone treatment was qualitatively different from non-thermal DBD plasma. They concluded that ozone

[1] According to conversion factors found on http://www.ozonesolutions.com/info/ozone-conversions-equations.

treatment did not play a role in the observed effects of plasma on mammalian cells.

Hence, the role of ozone and more broadly, the role of reactive oxygen species (ROS) in plasma sterilization is still widely debated. This paper concentrates on isolating and examining the role of ozone in DBD surface plasma sterilization. DBD plasma devices operating at 14 kHz and low input voltage are used to generate plasma. These plasma devices are enclosed within acrylic sterilization chambers of different volumes. Rates of production/decay of ozone during and after plasma generation using these devices are measured. The dependence of this rate of production/decay on the volume of the sterilization chamber is also examined. Additionally, different substrates inoculated with *E. coli* are exposed to the ozone produced during plasma generation. In doing so, the average ozone levels as well as exposure times required for significant reduction in bacterial concentration are determined. When ozone production during plasma generation is inhibited through two different methods, the reduction in *E. coli* concentration is not significant leading us to conclude that ozone produced during plasma generation is indeed responsible for bacterial inactivation. The remainder of the paper is written as follows: Section 2 lists the experimental protocols and materials used. Section 3 presents and discusses the results of the various studies described above and Section 4 draws conclusions.

2. Experimental Protocols

2.1. Plasma Generation and Diagnostics

The experimental setup used for DBD plasma generation in this paper has been described in detail in a previous paper.[3] The plasma device consists of a dielectric layer (≈1.6 mm thick), either side of which an electrode is embedded. Two types of dielectric material are tested: FR4 (flame retardant 4) and a hydrocarbon ceramic laminate (Rogers® 3003 C), which will henceforth be known as semi-ceramic (SC). FR4 is commonly used for making printed circuit board and has a dielectric constant (ε) of 4.7, while SC has a dielectric constant of 3.00 ± 0.04 (according to manufacturer specs). The electrodes embedded on either side of this dielectric layer are made of copper coated with a tin finish. The top (powered) electrode has a comb-like pattern as shown in Figure 1 and is exposed to the air. The bottom (grounded) electrode is a square sheet and measures the same in surface area as the top electrode ($2.4 \times 2.4\,cm^2$) and is not exposed to air during plasma generation.

To generate plasma, as shown in Figure 1 above, a sinusoidal wave of 14 kHz frequency is amplified such that the final input signal being fed into the top (powered) electrode measures 12 kV peak–peak (unless otherwise mentioned). The potential difference between the top and bottom electrodes leads to DBD plasma generation on the surface of the comb-like electrode, as shown in Figure 1.

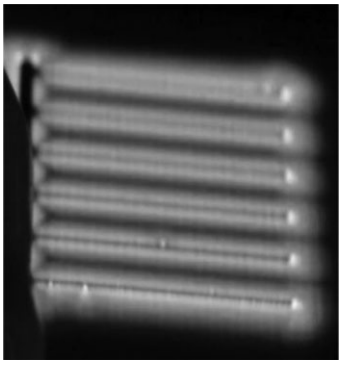

Figure 1. An image of the top (powered electrode) of the DBD plasma device, during plasma generation.

Ozone levels during and after plasma generation are measured using a 2B Tech® Ozone Monitor (Model 202). Measurement of ozone is based on absorption of UV light (at 254 nm) and subsequent comparison of the quanta of light reaching the detector before and after absorption by ozone. Ozone levels are measured in units of ppb (or ppm). Air inside the chamber is sampled every 10 s and measured ozone levels are saved to a computer via a LabView® interface.

2.2. Microbiological Testing

Cultures are maintained frozen at −80 °C in broth with 25% glycerol and inoculated onto fresh plates weekly. *E. coli C600* is grown on Luria-Bertani (LB) agar or broth at 37 °C. Before each experiment, the optical density (OD) of the microbial sample is measured using an Ultrospec 10 cell density meter (GE Healthcare Bio-Sciences Corp., Piscataway, NJ) to estimate the density of the culture. An OD of 1 corresponds to approximately 5×10^8 colony forming units (CFU). Cultures are diluted as needed to ensure that approximately 10^6 CFU are inoculated onto any device. For each experiment, the plasma devices are inoculated with 20 μl of *E. coli* sample spread uniformly over the entire electrode surface area with a sterile inoculating loop. Only the top (powered) electrode of each plasma device is inoculated. After an experiment, the number of remaining test organisms left on each device is determined by spreading serial dilutions on appropriate agar plates as described. Plate counts are also performed on the inoculum to determine the exact concentration of organisms and an inoculated device not exposed to ozone is processed as control for the loss of viable counts due to drying or adherence to the device. Experiments are performed in triplicate unless otherwise noted.

3. Results and Discussion

3.1. Characterization of Trends of Ozone Production/Decay During DBD Plasma Generation

In order to study the trend of ozone production/decay during and after DBD plasma generation, a clean FR4

DOI: 10.1002/ppap.201300108

plasma device is enclosed in acrylic sterilization chambers of different volumes. In each chamber, the plasma device is placed, powered for 2 min (120 s) and then allowed to rest for an additional 5 min (300 s). Ozone levels are measured every 10 s throughout this 7 min (420 s) interval. The ozone probe used to sample ozone levels is placed 2.5″ above the chamber floor and 5″ to the right of the device (measured from the center-point of the device).

The dimensions of each of these chambers are given below. Here l, b, and h denote length, breadth, and height respectively.

- Chamber #1 – $l = 12''$; $b = 10''$; $h = 7'' - 840\ \text{in}^3$.
- Chamber #2 – $l = 12''$; $b = 10''$; $h = 14'' - 1\,680\ \text{in}^3$.
- Chamber #3 – $l = 24''$; $b = 10''$; $h = 14'' - 3\,360\ \text{in}^3$.
- Chamber #4 – $l = 48''$; $b = 23.5''$; $h = 24'' - 27\,072\ \text{in}^3$.

Thus, Chamber #2 is twice as high as Chamber #1 and Chamber #3 is twice as long as Chamber #2. Chamber #4 is huge in all three dimensions, as compared to the other three chambers. The volume ratio of the chambers is 1:2:4:32 with respect to the smallest chamber (#1). Three types of aspect ratios (AR) can be defined for these chambers – l:b, l:h, and b:h denoted by AR_1, AR_2 and AR_3, respectively For Chamber #2 and #3, AR_3 is the same while AR_1 and AR_2 for Chamber #3 are double that of Chamber #2. Figure 2 shows the production/decay profiles obtained in this manner for all four sterilization chambers using the same DBD device.

In Figure 2, seven different plots are shown. The first four plots (only markers) show the variation of measured ozone concentrations throughout the 7-min (420 s) interval in the four different chambers. For these four plots, error is plotted as standard deviation of measured ozone levels at each time point. A closer study of these four plots enables the identification of three distinct phases during and after plasma generation in each chamber. These three distinct phases are labeled in the figure as the ozone production phase, the ozone diffusion phase, and the ozone decay phase. In the production phase, while plasma is generated for 2 min (120 s), measured ozone concentrations show a gradually increasing trend. As soon as the plasma is turned off at 120 s, a sharp dip in measured ozone concentration is observed from Figure 2. This sharp decrease in measured ozone concentration lasts for a very short time (30 s) and is therefore identified as the diffusion phase. After 160 s, Figure 2 shows that the measured ozone concentration in each chamber gradually begins to decrease (as opposed to the sharp reduction in ozone concentration at 120 s). Appropriately, this phase is identified as the decay phase. Essentially, in this phase, produced ozone slowly decomposes. Diluted ozone at room temperature is quite stable[10] and hence decomposes on the timescales of minutes. We delineate the two phases after $t = 120$ s as diffusion and decay (or decomposition) phase based on the timescales of decrease in ozone concentrations. During the diffusion phase, a very sharp reduction in ozone concentration occurs whereas during the decay phase, the decrease in

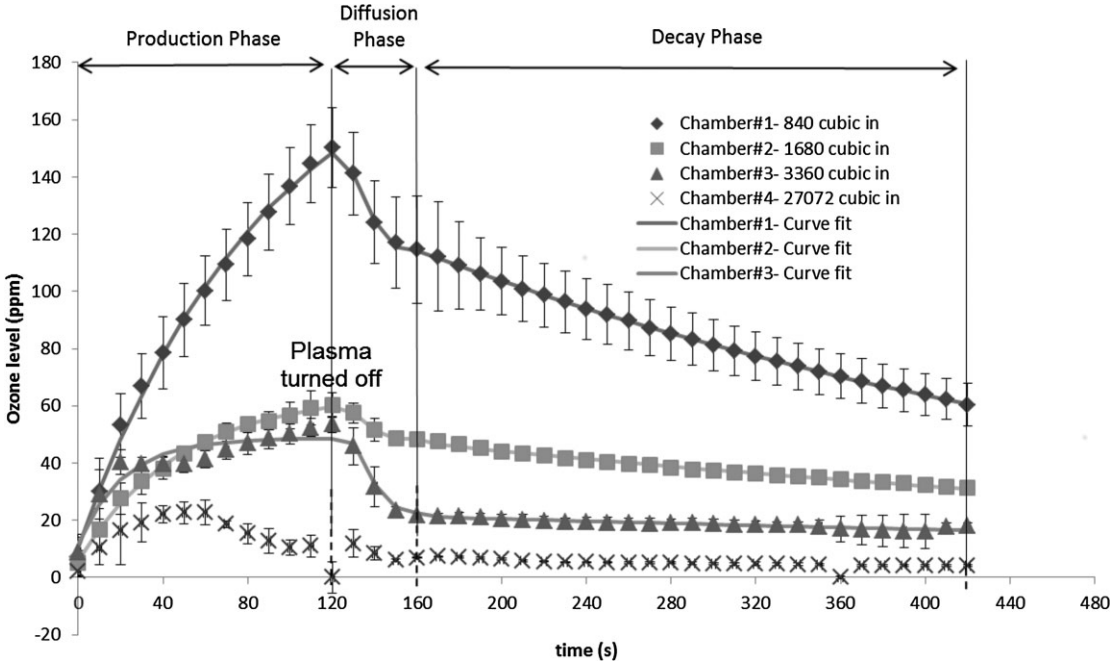

Figure 2. Comparison of ozone concentrations produced during and after plasma generation in all four chambers. Plasma device is powered at 0 s and turned off at 120 s, after which setup is allowed to rest for another 300 s.

Table 1. Values of the constants used in Equation (5a–c).

Chamber #	a [ppm]	b [ppm]	c [s]	D [ppm s^{-2}]	$[O_3]_0$ [ppm]	τ [s]
1	197	186.4	89.13	0.073	168.8	410
2	64.85	58.57	47.78	0.028	31.3	618.047
3	48.66	36.72	21.4	0.062	24.91	1 017.087

ozone concentration is gradual. The timescale of reduction in ozone concentration is similar to reported trends[11] leading us to believe that the sudden decrease in ozone concentrations during the diffusion phase is more likely due to flow effects (discussed later).

Analyzing the measured ozone concentrations in each phase, using trend-fitting tools, each phase can be further identified by a characteristic equation. These Equation (5a–c) are listed below.

$$\text{Production phase} \quad [O_3] = a - be^{-t/c} \qquad 0\,\text{s} \le t \le 120\,\text{s} \tag{5a}$$

$$\text{Diffusion phase} \quad \frac{d^2[O_3]}{dt^2} = D\,(\text{ppm s}^{-2}) \qquad 120\,\text{s} < t \le 160\,\text{s} \tag{5b}$$

$$\text{Decay phase} \quad [O_3] = [O_3]_0 e^{-t/\tau} \qquad 160\,\text{s} < t \le 420\,\text{s} \tag{5c}$$

In the above equations, $[O_3]$ is the calculated ozone concentration and $[O_3]_o$ is the ozone concentration present initially at the beginning of the decay phase. Both are expressed in units of ppm, where 1 ppm is equal[2] to a density of 2.648×10^{13} cm^{-3}. In Equation (5a) (production phase), "a" and "b" are production coefficients (ppm) while "c" is the production time constant (seconds). In Equation (5b) (diffusion phase), "D" is the diffusion coefficient (ppm s^{-2}). In Equation (5c) (decay phase), "τ" is the decay time constant (seconds). The values of all these coefficients and time constants for each chamber except Chamber #4 are listed below in Table 1. Calculating and plotting the ozone concentration versus time using these equations for Chambers #1–#3 gives rise to the latter three plots shown in Figure 2, denoted by the word "curve fit" at the end.

In Figure 2, it is observed that ozone concentrations calculated using Equation (5a) agree very well with measured ozone concentrations in the case of Chambers #1 and #2. However starting with Chamber #3, the measured ozone concentrations start to deviate from the expected trend. This deviation is very prominent in the production phase for Chamber #3. As mentioned before, Chamber #3 is twice as long as Chamber #2 or #1. Thus it seems that compared to Chamber #1, increasing the height of the chamber does not affect the expected trend of ozone concentrations, but increasing the length makes it more difficult to accurately predict the ozone concentrations according to Equation (5a). This is why coefficients or constants have not been calculated for Chamber #4, due to its much larger proportions as compared to the other chambers.

Plotting the measured ozone levels with the corresponding chamber volume, at different time points during the 7-min (420 s) interval produces a correlation such as the one given below in Figure 3. In Figure 3, Figure 6 time points have been plotted: 60 s, 120 s (during the production phase), 160 s (during the diffusion phase) and 240, 360, and 420 s (during the decay phase). Both chamber volume (X-axis) and ozone levels (Y-axis) are plotted on a log 2 scale for easier comparison.

There are some interesting points to be noted in Figure 3. First as expected, at all times, measured ozone concentration in Chamber #1 is the highest. Secondly, during the production phase, it seems that measured ozone levels at 60 and 120 s for both Chambers #2 and #3 are similar. Even from Figure 2, observing ozone measurements during the production phase for Chambers #2 and #3, it is noted that the values for both chambers are very similar. Again, for Chambers #2 and #3, AR_3 is the same while AR_1 and AR_2 for Chamber #3 are double that of Chamber #2. Thus, the similar levels of ozone noted during the production phase for Chambers #2 and #3 in Figure 3 imply that the ozone produced during the production phase is dependent on AR_3. Once the plasma is turned off, both in the diffusion phase and the decay phase, Figure 3 once again reinforces the dependence of measured ozone concentrations on the volume of the sterilization chamber.

However, this brings up another important point. The same clean FR4 device, when operating at the same input voltage and frequency (i.e., same input power), when placed in different chambers gives rise to different concentrations of measured ozone in each chamber. As the ozone is being produced during the production phase, the smallest chamber leads to confinement of the produced ozone, hence enabling the ozone probe to detect it in

[2]According to conversion factors found on http://www.lenntech.com/calculators/ppm/converter-parts-per-million.htm.

DOI: 10.1002/ppap.201300108

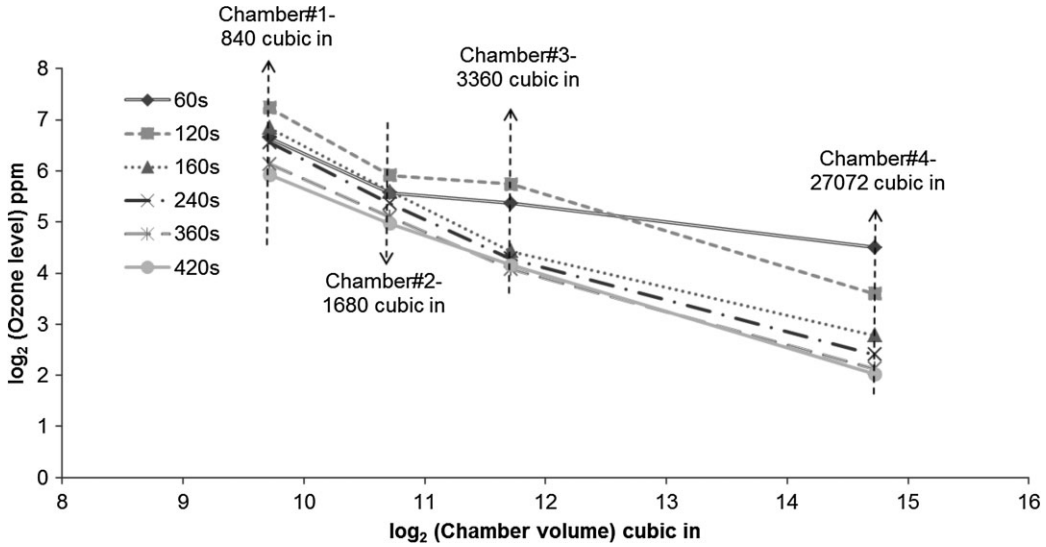

Figure 3. Correlation of measured ozone levels with chamber volumes. The different plots at time points (60, 120, 160, 240, 360, and 420 s) represent ozone measurements in each chamber at that particular time point.

very high concentrations. However as the volume of the chamber is increased, the produced ozone has more and more volume to diffuse (or spread) into. Thus, an ozone probe placed at the exact same position in each chamber begins to detect lesser and lesser concentrations of ozone as the chamber volume increases. However from the discussion of expected trends above (Equation 5a–c), it seems that the length of the chamber is more important in determining how the ozone produced during the production phase diffuses inside the chamber, i.e., longer the length, higher the spread of produced ozone and more difficult it is to predict the expected ozone concentrations.

Much of the discussion of the results in Figure 2 and 3 indicate that the measurement of ozone concentration during and after plasma generation is highly dependent on the chamber volume. Since ozone levels discussed here are being measured using a single ozone probe at a single position, it is also important to evaluate the dependence of measured ozone levels on the position of the ozone probe.

In order to do this, a plasma device is placed in the largest Chamber #4. The device is powered over a time interval of 2 min and the ozone levels at different locations (along both the *X*-axis and *Y*-axis) of the chamber are measured. The various locations at which ozone is measured inside the chamber are shown in Figure 4. For all measurements in Figure 4, the ozone probe is positioned at a height of 5″ above the floor of the chamber.

The aim of such an experiment was to get an idea of the spatial variation of ozone levels inside Chamber #4. This spatial variation is given below in Figure 5a and b. Figure 5a shows the spatial variation of ozone production along the *X*-axis of the chamber while Figure 5b shows the spatial variation of ozone production along the *Y*-axis of the chamber. While ozone data is sampled every 10 s, for the sake of simplicity only the data sets at 30, 60, 90, and 120 s have been plotted and shown.

Figure 5a demonstrates that the highest amount of ozone is produced in the upper right quadrant of the chamber (as labeled in Figure 4). Typically, the levels of ozone noted on the right hand side (RHS) of the chamber are more than those on the left hand side (LHS). Figure 5b indicates that the distribution of ozone produced along the *Y*-axis does not follow a clear-cut trend, as along the *X*-axis. This bias in ozone levels toward the RHS of the

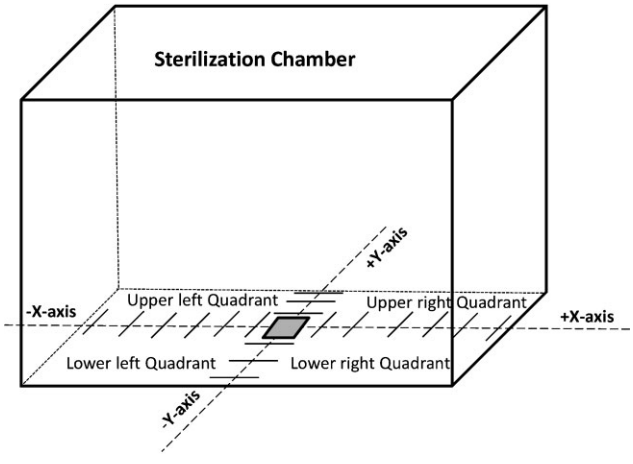

Figure 4. Schematic of Chamber #4. The gray square in the middle represents the plasma device. The black short lines represent the different locations at which ozone measurements are taken. These locations are uniformly spaced (4″ apart), along the *X*- and *Y*-axis.

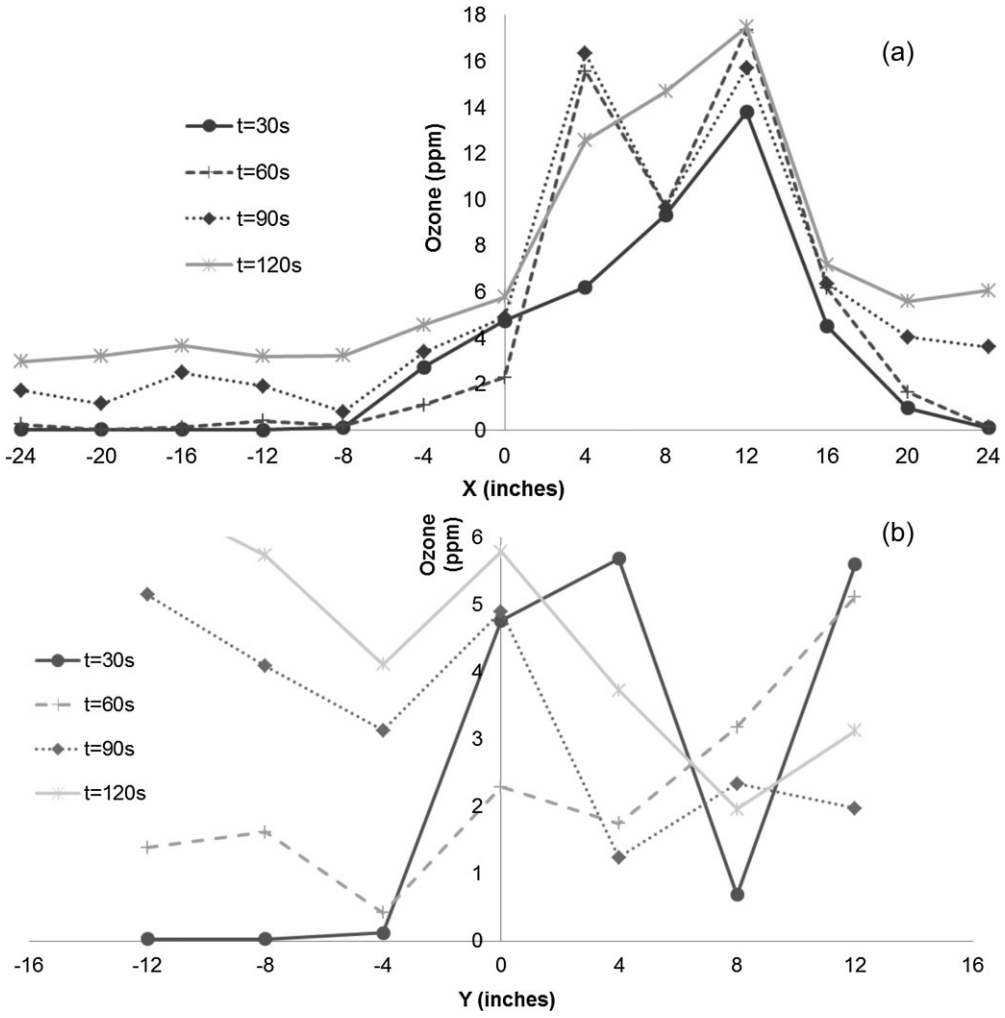

Figure 5. Spatial variation of ozone distribution inside the sterilization chamber. (a) Along the *X*-axis. (b) Along the *Y*-axis.

chamber can be explained due to the directional bias of the electrodynamic body force ($\vec{F} = q\vec{E}$) produced as a result of the plasma generation, where "F" is the electrodynamic force, "q" is the charge and "E" is the produced electric field. Previous research conducted by our group[17,18] elucidates further on the generation of this electrodynamic force and its dependence on the various plasma input parameters as well as its effect on fluid momentum. Most importantly, the direction of this force is from the powered electrode to the grounded electrode. Because of this electrodynamic force (from left to right), the flow is "pushed" to the right, as shown in Figure 6a. When

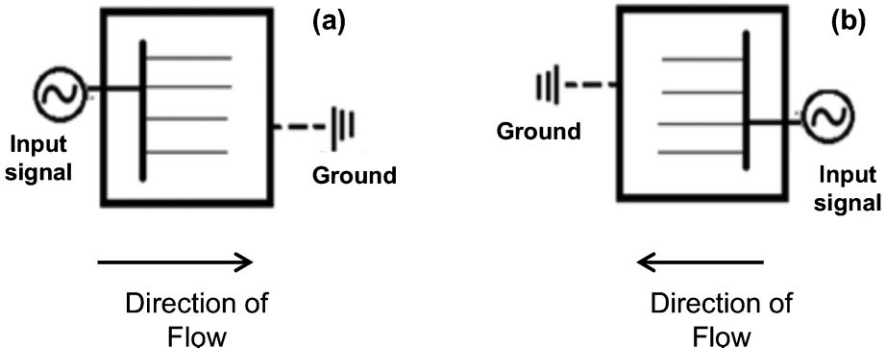

Figure 6. (a and b) The two different configurations in which the device is placed. It is noted that in (a), flow is "pushed" toward the right (along the *X*-axis). In (b), when the configuration is flipped, flow is "pushed" toward the left.

DOI: 10.1002/ppap.201300108

the configuration is flipped, as shown in Figure 6b, the direction of force is from right to left and thus the flow would be pushed to the left in such a configuration.

This "pushing of the flow" effect may also explain the sudden dip in ozone concentrations in the diffusion phase (Figure 2). During plasma generation, the ozone levels are continuously pushed toward the RHS of the chamber. However at 120 s, as soon as plasma is turned off, due to the sudden absence of a "pushing force," produced ozone may diffuse out toward the LHS of the chamber, thus causing a sudden reduction in ozone concentrations.

In the above section, an overview of the trends of ozone production/diffusion/decay during DBD plasma generation is provided. Once a FR4 plasma device is powered for 2 min (120 s) and left to rest, a plot of the produced ozone concentrations versus time can be divided into three distinct phases: production, diffusion, and decay. Each of these phases can be defined by a characteristic equation. However the predictability of measured ozone concentrations according to these characteristic equations is dependent on the chamber dimensions. As the length of the chamber increases, it becomes more difficult to predict ozone concentrations using these characteristic equations. Ozone concentrations measured during each phase are also dependent on chamber dimensions. Three ARs, AR_1–AR_3 have been defined. Results (Figure 2–3) show that during the production phase, ozone concentrations are dependent on AR_3 but during diffusion and decay phases, they are dependent upon AR_1. Not only are these measured ozone concentrations dependent upon chamber volume, but also upon the placement of the ozone probe (Figure 5–6).

Hence, it is apparent that any substrate inoculated with *E. coli* and placed at one constant position in each chamber is exposed to varying concentrations of ozone. The next section focuses on understanding the effect of exposing *E. coli* concentrations to the produced ozone.

3.2. The Effect of Ozone Produced During DBD Plasma Generation on *E. coli*

DBD plasma generation produces a plethora of species: UV photons, charged particles, and neutrals. The role of each of these species in the mechanism of plasma sterilization is highly debated. However, one major factor that has been considered is the ROS produced during DBD plasma generation. Since DBD plasma produces high concentrations of ozone, it is necessary to first isolate and evaluate the role of ozone in plasma sterilization.

To do so, different substrates are inoculated with *E. coli* (20 μl corresponding to 10^6–10^8 CFU) and placed next to a clean plasma device generating plasma. Both inoculated and clean devices are placed inside Chamber #1. The schematic for such tests is shown in Figure 7.

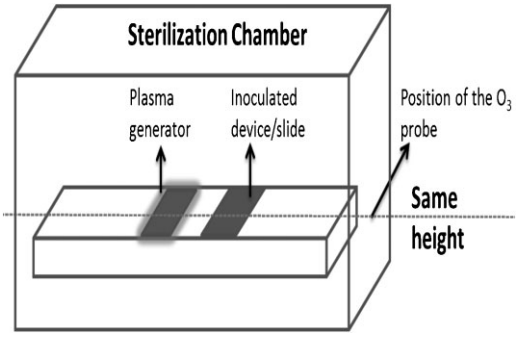

Figure 7. Experimental schematic for the exposure tests. On the left is the plasma generator, which is used to generate plasma and produce ozone inside the chamber. On the right is the inoculated device/glass slide, which is inoculated with 20 μl of *E. coli* and exposed to the ozone produced by the plasma generator.

In the schematic below, the "plasma generator" is the clean plasma device generating plasma and thus, ozone for the required time. The "inoculated device/slide" represents the substrates inoculated with *E. coli*. Two types of plasma generators are tested: FR4 and SC plasma devices. Three types of inoculated substrates are tested: a FR4 plasma device, a SC plasma device, and a glass cover-slide. The inoculated substrates are *not* exposed to direct plasma, but instead to the reactive species produced during plasma generation, especially ozone. Judging by ozone distributions in Figure 5, the ozone probe is positioned on the RHS of the chamber and about ≈1″ away from the inoculated device.

On comparing measured ozone concentrations during and after plasma generation, it is observed that the ozone production in the case of FR4 is marginally higher than that in the case of SC. This comparison is shown in Figure 8. In Figure 8, similar production/diffusion/decay phases are noted in the case of SC plasma devices. It is noted that the average ozone concentration in the case of FR4 is ≈26.05% higher than in the case of SC.

The three kinds of inoculated substrates described above are exposed individually to ozone produced by both a FR4 and SC plasma generator for 7 min (420 s). During this 420 s interval, plasma is generated (i.e., ozone is actively produced) for 2 min (120 s) and for the rest of time, the inoculated substrate is simply exposed to the residual ozone concentrations. The results of such an experiment are given in Figure 9.

In Figure 9a, N denotes the number of *E. coli* survivors after ozone exposure. Error is listed in terms of the standard deviation of the mean of $\log_{10}(N)$ over a number of trials. A single $\log_{10}$ reduction implies a 1/10th decrease in *E. coli* concentration, i.e., 10^7 CFU reduces to 10^6 CFU. Initial concentration of *E. coli* is ≈10^8 CFU. In Figure 9a, for the FR4 plasma generator, two additional exposure

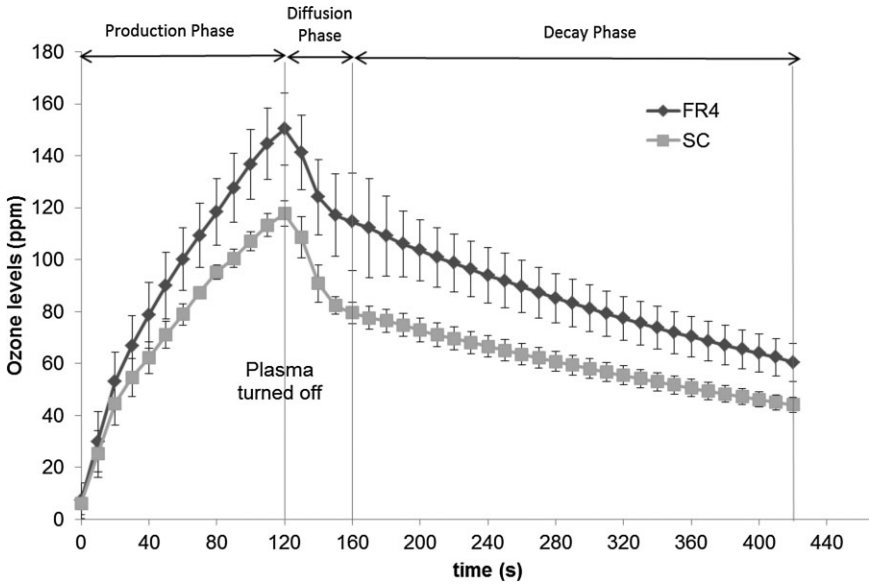

Figure 8. Comparison of ozone production during 7 min (420 s) for FR4 versus SC. The plasma device is powered at 0 s and turned off at 120 s, after which the setup is allowed to sit for another 300 s.

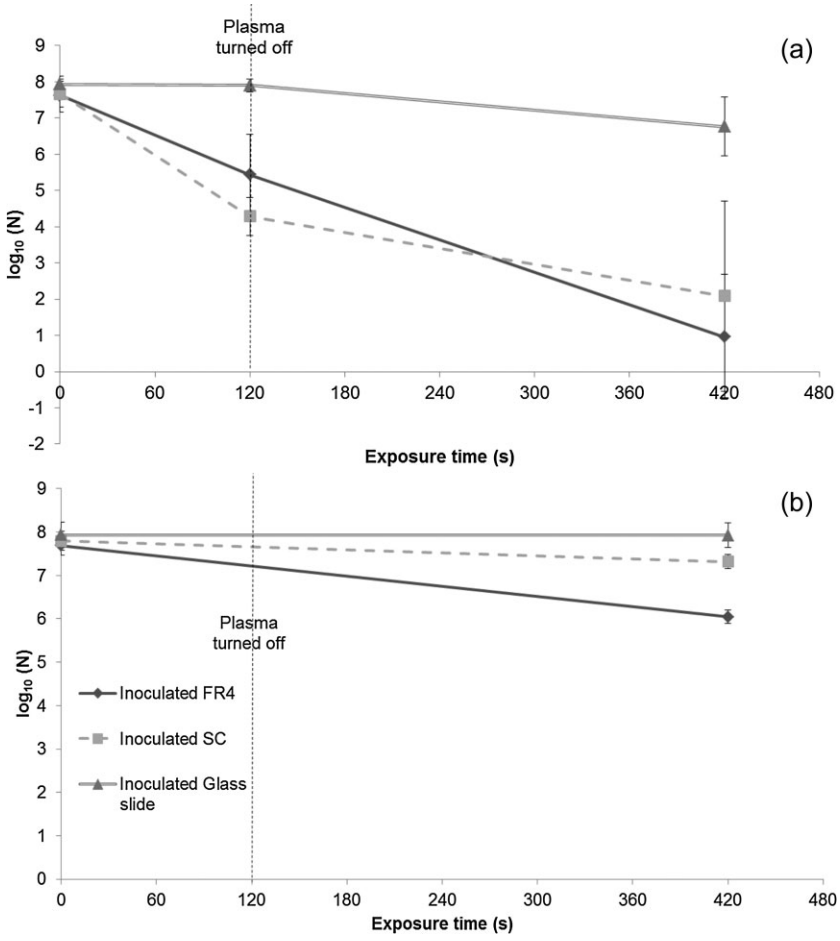

Figure 9. Inactivation plots due to ozone exposure with (a) FR4 plasma generator and (b) SC plasma generator.

DOI: 10.1002/ppap.201300108

times were tested: 2 and 32 min. The results for the 2-min time point are shown in Figure 9a while the results for the 32-min time point are not shown. It is observed that after 7 min of ozone exposure using a FR4 plasma generator, *E. coli* concentrations in the case of the inoculated FR4 and SC plasma devices are significantly reduced. *E. coli* concentrations in the case of the inoculated glass slide are not affected significantly. Even after a 32-min exposure using a FR4 plasma generator, *E. coli* concentrations are completely inactivated in the case of inoculated FR4/SC plasma devices and not significantly affected in the case of inoculated glass slide. However as is evident from Figure 9b, when inoculated substrates are exposed to ozone concentrations produced using a SC plasma generator, *E. coli* concentrations are not affected significantly.

The average ozone concentration is derived by calculating the average of measured ozone levels over a 420 s interval and is used as an empirical parameter to compare the dependence of bacterial inactivation on ozone concentrations. During a 7-min interval of exposure, any inoculated substrate is exposed to an average of ≈90 ppm of ozone in the case of FR4 plasma generator as compared to an average of ≈67 ppm of ozone in the case of SC plasma generator. Thus, an average of ≈90 ppm of ozone is required for significant reduction (7 $\log_{10}$) in *E. coli* concentrations exposed to ozone produced during DBD plasma generation.

In the case of inoculated glass slides, *E. coli* concentrations are not significantly affected by ozone exposure, using both a FR4 plasma generator as well as a SC plasma generator. This indicates that the effect of ozone on *E. coli* is also dependent on the type of substrate used for inoculation. When glass slides are inoculated with 20 μl of *E. coli*, it is visibly evident that the bacterial sample deposited on the glass slide clumps into random droplets on the surface of the glass slide. This is because glass is a far less hydrophilic surface than FR4 or SC, thus making it difficult for liquid to adhere to it. Hence this uneven clumping of *E. coli* on the glass slide might be leading to shielding of the underlying bacteria, which explains the insignificant drop in bacterial concentration in the case of glass slides.

Figure 10 below shows inactivation results obtained when the same ozone exposure experiment is repeated with an inoculated FR4 plasma device, using a FR4 plasma generator in different chambers. When an inoculated FR4 plasma device is placed at a constant position in different chambers and exposed to ozone produced during plasma generation, the inoculated substrate is exposed to varying levels of ozone.

Again, *E. coli* concentrations in Chambers #2–#4 are reduced only by 1–3 $\log_{10}$. *E. coli* concentrations are only significantly reduced (7 $\log_{10}$) in Chamber #1. *E. coli* concentrations are exposed to average ozone concentrations of ≈90, 41, 27, and 9 ppm in chambers #1–4 respectively over a 7-min (420 s) interval. Thus bacterial inactivation results from both Figure 9 and 10 indicate that there is a threshold level of ozone required for injuring *E. coli* lethally.

The next step was to evaluate whether ozone produced during plasma generation is truly responsible for the bacterial inactivation noted in Figure 9a and 10. In order to evaluate this, ozone produced was inhibited in the following two ways: (i) using activated charcoal to inhibit ozone production and (ii) generating plasma using N_2 as the discharge gas.

A fixed amount of activated charcoal (MarineLand Black Diamond®) is placed on the plasma generator and the plasma generator subsequently operated. In doing so, the produced ozone is directly adsorbed by the charcoal and ozone levels are immediately reduced by around 98%. For subsequent tests, care is taken to adjust this amount of activated charcoal on the plasma device to maintain the same reduced levels of ozone.

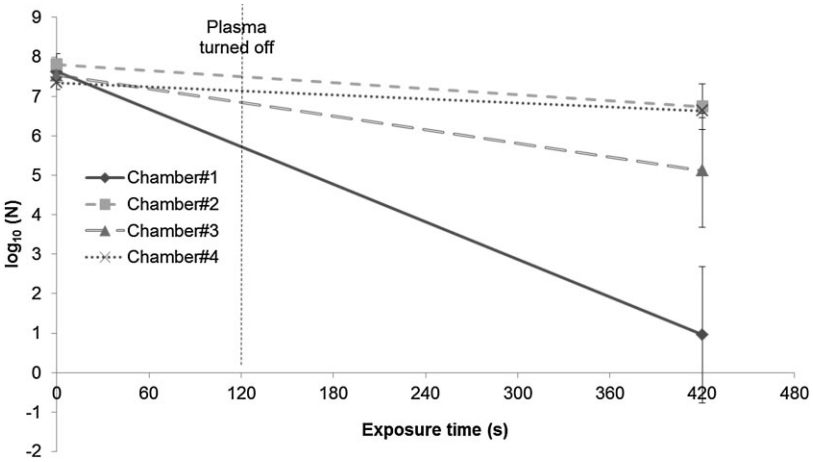

Figure 10. Inactivation plots due to ozone exposure in the different chambers using a FR4 plasma generator and an inoculated FR4 substrate.

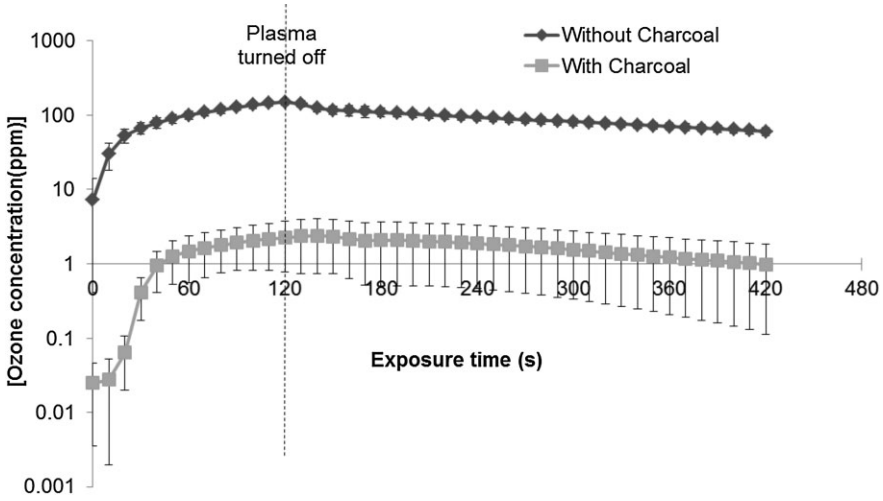

Figure 11. Comparison of ozone production with and without charcoal for Chamber #1. Ozone concentration on the *Y*-axis is shown on a $\log_{10}$ scale.

This comparison of levels of ozone produced with and without charcoal for Chamber #1 is shown in Figure 11. For both cases, a clean FR4 plasma device is placed in Chamber #1, powered at 0 min and turned off at 2 min (120 s), after which the setup is allowed to rest for another 5 min (300 s). Since there is a huge difference between ozone levels in both cases, for the sake of simplicity, ozone concentration (on the *Y*-axis) is shown on a logarithmic scale.

As is evident from Figure 11, the addition of charcoal on top of the device during plasma generation leads to a reduction of ozone concentration by a factor of 100. For all the sterilization tests testing the effect of exposing *E. coli* concentrations to ozone produced in cases with and without charcoal, the amount of charcoal on the device was adjusted to maintain the reduced ozone concentration as shown in Figure 11.

As per protocol, an inoculated FR4 plasma device is placed next to the plasma generator (a clean FR4 device) covered with charcoal. For the purpose of this paper, such a configuration will be referred to as a "modified plasma generator." Chamber #1 is used for these tests.

When the inoculated substrate is exposed to this modified plasma generator for 7 min (420 s) and then post-processed, negligible reduction in *E. coli* concentration is observed, thus proving that the ozone produced during plasma generation is responsible for inactivation of *E. coli*. This inactivation effect with and without charcoal, in the case of an inoculated FR4 substrate, is shown in Figure 12. The wide disparity in bacterial inactivation is immediately evident and proves that the reduced ozone concentrations due to adsorption by activated charcoal do not have as lethal an effect on *E. coli*, when compared to the case of no charcoal. While Figure 11 demonstrates that ozone produced during DBD plasma generation is responsible for bacterial inactivation, an alternative experiment to prove this was also conducted.

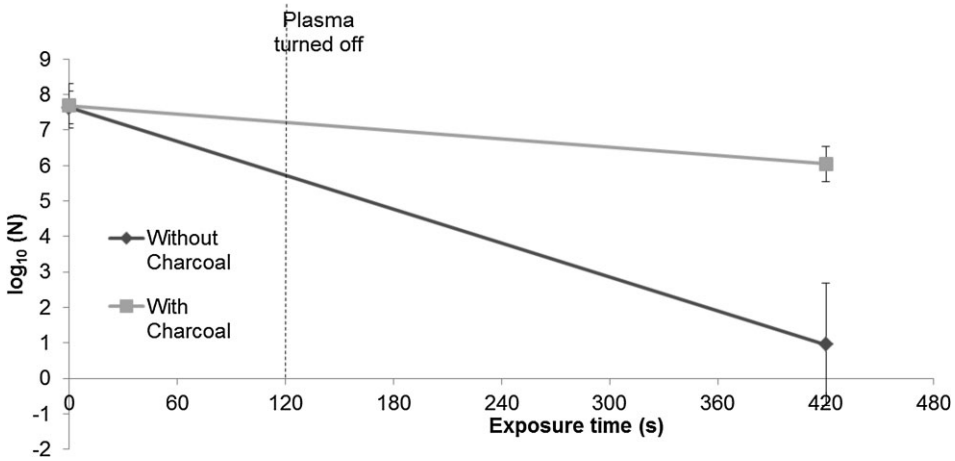

Figure 12. Sterilization curve with and without charcoal.

DOI: 10.1002/ppap.201300108

DBD Plasma is generated using N_2 as the working gas. For the same device, plasma generation parameters such as input frequency and voltage, and thus the generated electric field, are kept similar. A smaller vacuum chamber ($9.3'' \times 7.4'' \times 5.6''$) is used as the sterilization chamber. The chamber is then evacuated to an absolute pressure of 0.0978 atm, following which N_2 gas (Airgas, Inc., UN1066, 99.0% N_2) is introduced into the chamber until the pressure in the chamber is restored to atmospheric pressure. This process is repeated four times to maintain a majority N_2 environment. The aim of such an intensive method of flushing out all the air and filling the chamber with N_2 is to ensure that very low O_2 levels remain in the chamber in order to inhibit ozone production during DBD plasma generation. Using laws of partial pressures, this percentage of N_2, at the end of four flushes is calculated to be $99.998 + 0.78\%$. Hence the aim of maintaining a pure N_2 environment is accomplished fairly well.

The experimental protocol in these tests, unlike the previous ozone exposure tests, consists of inoculating select FR4 devices with 20 μl of *E. coli* (initial concentration $= 10^8$ CFU), placing them in the sterilization chamber, sealing the chamber, flushing the chamber with N_2 four times and then powering the device for the requisite time interval (Δt). Owing to the rigorous nature of these tests, only FR4 substrate is tested. The time intervals tested are $\Delta t = 60$ s, 120 s. Each time interval test is replicated thrice, using the same *E. coli* sample to ensure repeatability. The comparison of sterilization results from plasma generation using discharge gas as air versus N_2 is given below in Figure 13.

In Figure 13, in the case of air, complete bacterial inactivation is noted within 120 s. In the case of N_2, starting from an initial concentration of 10^6 CFU, at the end of 120 s of plasma generation, only a $1 \log_{10}$ reduction in *E. coli* concentration is noted. However, the initial concentration of *E. coli* used is 10^8 CFU, which leads us to conclude that the flushing of the chamber four times as well as evacuation of the chamber to extremely low pressures causes a $2 \log_{10}$ reduction in *E. coli* concentration. Nevertheless, even with a pre-plasma concentration of 10^6 CFU, it is evident that plasma generation in N_2 (hence, plasma generation in the absence of ozone) does not cause much of a reduction in *E. coli* concentration. Thus from the results of the charcoal tests as well as N_2 tests, we conclude that ozone produced during plasma generation is capable of inactivation of *E. coli*, on prolonged exposure times.

Plasma generation in air produces a huge number of reactive chemical species (both neutral molecules and charged particles). Our experimental setup measures concentrations of one of these reactive chemical species, i.e., ozone. Since ozone is produced in such great quantities during DBD plasma generation, it is prudent to ask what role it plays in DBD plasma sterilization. In order to do that, results with experiments involving the exposure of *E. coli* to ozone generated during and after plasma production are discussed. From the results of these experiments, it is evident that a threshold level of ozone is required to kill *E. coli*. This threshold level is calculated to be an average ozone concentration of 90 ppm. Consequently, the next prudent question to ask is whether the obtained results indicate that the observed reduction in bacterial concentration is due to the produced ozone. Inhibiting produced ozone (using activated charcoal) and repeating exposure experiments leads to insignificant reduction in *E. coli* concentrations, proving that ozone produced during and after plasma exposure is indeed responsible for inactivating *E. coli*. Additionally generating DBD plasma at atmospheric pressure in a N_2-filled environment, using inoculated FR4 devices proves that sterilization due to DBD plasma in a N_2-filled environment is not as effective as sterilization due to DBD plasma in air. This not only reinforces the theory

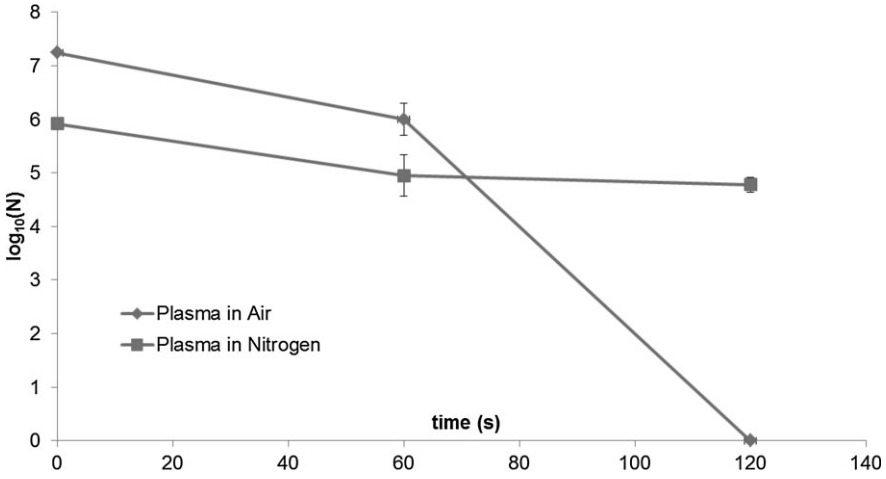

Figure 13. Plasma sterilization curve, using air and nitrogen as the working gases.

that the reduction of ozone (all the air in the chamber is evacuated and filled with N_2) leads to insignificant reduction in *E. coli* concentrations but also proves that N_2, which is a major component of air and a prominent peak on the spectroscopic signature[3] does not play a dominant role in DBD surface plasma sterilization.

However from Figure 9, it is evident that after 2 min of exposing *E. coli* concentrations to produced ozone, a 3–4 $\log_{10}$ reduction is obtained, starting from an initial concentration of 10^8 CFU. We have shown previously[3] that 2 min of direct plasma treatment of *E. coli* using DBD surface plasma produces complete sterilization, starting from an initial concentration of 10^{6-7} CFU. Obviously the timescales of inactivation due to ozone exposure and inactivation due to direct DBD surface plasma treatment do not match. However, considering that during direct DBD surface plasma treatment, *E. coli* present on the surface of the DBD plasma device is directly exposed to produced ozone, it is possible that *E. coli* concentrations on the surface of the DBD plasma device are exposed to even higher levels of ozone as compared to an inoculated substrate placed ≈1″ away from the plasma generator.

At this time, the mechanisms of how activated charcoal reacts with and removes, if any, other ROS are not well understood. However, considering the lifetime of other ROS (milliseconds to seconds) as compared to ozone (minutes), experiments with inoculated substrates placed at a distance away from the plasma generating source substantiate the majority role of ozone in stimulating bacterial inactivation. Since the inoculated substrate is placed at a distance from the plasma generating source, ROS with their relatively short lifetimes will not be able to reach the inoculated substrate in time to cause inactivation. Future research in this area may detect and measure the concentrations of absorbed ROS giving insight into which (and how) other species produced during DBD plasma generation acts in synergy with ozone to produce complete sterilization.

Another way to characterize the produced ozone is by using an intrinsic parameter that is capable of predicting the ozone level produced by powering a plasma device with a certain set of input parameters. Additionally, this predicted ozone level should be independent of the volume of the sterilization chamber in which the device is enclosed. Consider an input voltage of 12 kV pp and an input frequency of 14 kHz used to power a clean FR4 plasma device in different chambers. The same device (same input power) is producing ozone in all four chambers.

Power "*P*" is calculated by the formula $P = 1/N \sum_{i=1}^{N} VxI$. Thus for a sterilization time of "*t*" seconds, the average absorbed input power over that interval can be calculated by the formula

$$P_{\text{ave}} = \frac{1}{N}\sum_{i=1}^{N} P_i \tag{6}$$

where $N = t/\Delta t$ and P_i is measured input power at a single time point. Thus for a sterilization time $t = 2$ min $= 120$ s, if power P_i was measured at intervals of 15 s, then $N = 120/15 = 8$. Once this average power is calculated, then the average power density (P_{den}) can be calculated by the formula

$$P_{\text{den}} = \frac{P_i}{A} \tag{7}$$

where A is the electrode surface area of the plasma device (≈5.76 cm^2). P_{den} is represented in units of W cm^{-2}.

Finally input energy flux (J cm^{-2}) is calculated by multiplying P_{den} with the treatment time.[19] The ratio of the measured ozone levels at each time point, divided by the surface area of the plasma device is further divided by the

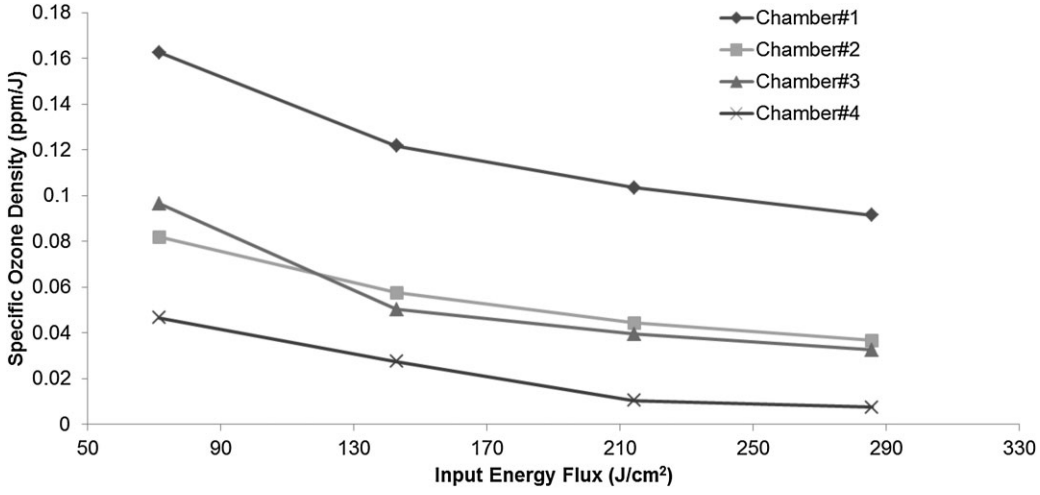

Figure 14. Comparison of specific ozone density versus input energy flux for the different sterilization chambers.

DOI: 10.1002/ppap.201300108

input energy flux at that particular time point for the same plasma device. This gives rise to specific ozone density (ppm J^{-1}). This specific ozone density is plotted versus input energy flux in Figure 14. In this figure, an almost-linear correlation is observed between the calculated specific ozone density and the calculated input energy flux. The average specific ozone density for Chambers #1–#4 are 0.12, 0.055, 0.054, and 0.023 ppm J^{-1}, respectively. This can be made further independent of volume of the sterilization chamber by dividing the average specific ozone density by the volume of the sterilization chamber. Thus given a device of a particular surface area, the above given trend should be able to identify and predict measured ozone concentrations, depending on volume of sterilization chamber. The input energy flux is also important in the context of sterilization. Complete sterilization of *E. coli* is observed at a threshold input energy flux of 280–290 J cm^{-2}. Thus future work will also concentrate on evaluating the significance of the specific ozone density in determining the point of complete sterilization, using the threshold input energy flux as an indicator.

4. Conclusion

The objective of this paper was twofold: (a) understand the lethality of ozone produced during plasma sterilization, using *E. coli* as the test pathogen and (b) understanding the role of ozone in the process of plasma sterilization itself.

The dissipation rates of ozone, during and after plasma generation using the different FR4/SC substrates as well as using chambers of different volumes, are determined. Three distinct phases are identified and the best-fit equations for each are given. The spread of ozone concentrations measured during each of these phases is shown to follow an aspect ratio (AR) dependence.

Ozone exposure tests are conducted in which an initial concentration of *E. coli* is exposed to ozone produced during plasma generation. Tests comparing the rate of inactivation using a FR4 and SC plasma generator determine a threshold value (≈90 ppm) required for significant reduction in *E. coli* concentrations. Furthermore, *E. coli* inactivation is shown to also depend on the type of substrate inoculated.

It was also necessary to prove that bacterial inactivation on exposure to air excited by plasma generation was due to the amount of ozone in this air, produced during plasma generation. In order to do so, two independent tests inhibiting ozone are conducted. In both of these tests, it is found that inhibiting ozone leads to ineffective bacterial inactivation.

However owing to the highly coupled nature of the problem, it is a little harder to understand the role of ozone in the process of plasma sterilization itself. Based on rates of bacterial inactivation following direct plasma exposure as compared to exposure to ozone produced during plasma generation, we conclude that while ozone plays a primary role in the process of plasma sterilization, it is not the only agent responsible for sterilization. Future work will involve trying to understand which other factor complements ozone production and enhances the sterilization process.

Acknowledgements: The authors are highly grateful to Sestar Medical for their generous financial support in funding this research. Sestar Medical had no role in study design, data collection and analysis, decision to publish, or preparation of the manuscript. Authors would also like to thank Raul.A.Chinga (Doctoral Candidate, Electrical Engineering, UF) for his constant help and support in manufacturing the plasma devices as well as his work on the plasma generation setup.

Received: August 20, 2013; Revised: September 18, 2013; Accepted: September 27, 2013; DOI: 10.1002/ppap.201300108

Keywords: dielectric barrier discharge (DBD); ozone; reactive oxygen species (ROS); sterilization; surface plasma

[1] H. Halfmann, B. Denis, N. Bibinov, J. Wunderlich, P. Awakowicz, *J. Phys. D: Appl. Phys.* **2007**, *40*, 5907.
[2] M. Laroussi, F. Leipold, *Int. J. Mass Spectrom.* **2004**, *233*, 81.
[3] N. Mastanaiah, J. Johnson, S. Roy, *PLoS ONE* **2013**, *8*, e70840.
[4] M. Kong, G. Kroessen, G. Morfill, T. Nosenko, T. Shimizu, J. Van Dijk, J. Zimmermann, *New J. Phys.* **2009**, *11*, 115012.
[5] E. Stoffels, Y. Sakiyama, D. Graves, *IEEE Trans. Plasma Sci.* **2008**, *36*, 4.
[6] M. Leduc, D. Guay, R. Leask, S. Coulombe, *New J. Phys.* **2009**, *11*, 115021.
[7] H. Ayan, G. Fridman, D. Staack, A. Gutsol, V. Vasilets, A. Fridman, G. Friedman, *IEEE Trans. Plasma Sci.* **2009**, *37*, 1.
[8] U. Kogelschatz, *Plasma Chem. Plasma Process.* **2003**, *23*, 1.
[9] B. Eliasson, M. Hirth, U. Kogelschatz, *J. Phys. D: Appl. Phys.* **1987**, *20*, 1421.
[10] A. Fridman, *Plasma Chemistry*, Cambridge University Press, New York **2008**.
[11] J. Wen, M. H. Thiemens, *J. Geophys. Res.* **1991**, *96*, 10911.
[12] W. Broadwater, R. Hoehn, P. King, *Appl. Microbiol.* **1973**, *26*, 391.
[13] N. Efremov, B. Adamiak, V. Blochin, S. Dadashev, K. Dmitriev, O. Gryaznova, V. Jusbashev, *IEEE Trans. Plasma Sci.* **2000**, *28*, 1.
[14] D. Dobrynin, G. Fridman, G. Friedman, A. Fridman, *New J. Phys.* **2009**, *11*, 115020.
[15] N. Vaze, M. Gallagher, S. Park, G. Fridman, V. Vasilets, A. Gutsol, S. Anandan, G. Friedman, A. Fridman, *IEEE Trans. Plasma Sci.* **2010**, *38*, 3234.
[16] S. Kalghatgi, A. Fridman, J. Azizkhan-Clifford, G. Friedman, *Plasma Process. Polym.* **2012**, *9*, 726.
[17] K. Singh, S. Roy, *J. Appl. Phys.* **2007**, *101*, 123308.
[18] K. Singh, S. Roy, *J. Appl. Phys.* **2008**, *103*, 013305.
[19] S. Kalghatgi, C. Kelly, E. Cerchar, B. Torabi, O. Alekseev, A. Fridman, G. Friedman, J. Azizkhan-Clifford, *PLoS ONE* **2011**, *6*, e16270.